Nighttime Radiative Cooling of Low-slope Roof Systems

Mathew P. Dupuis
Structural Research Inc.
Middleton, Wis.

Keywords

Roof, temperature, cooling, night, surface

Abstract

Nighttime radiative cooling of roof systems is a phenomenon that occurs every night. The net effect of this process is that roof membranes cool below the ambient air temperature. The amount of cooling and temperature differential that develops depends on multiple factors.

This paper uses field data collected from the Midwest Roofing Contractors Association (MRCA) test bed project in Manhattan, Kansas, which has TPO, EPDM, PVC and polymer-modified bitumen membranes present. The membranes have had thin-film photovoltaic (PV) panels adhered to them; each of these membranes and PV panels has been instrumented for temperature with thermocouples placed directly below the membrane. In addition, the MRCA site has a suite of weather and radiometric sensors to record the net energy exchange taking place every day.

Discussion within the paper includes details of the sensor system, history of research in the area of radiative cooling, theory of the energy exchange taking place, charts of field data, maximum observed temperature differentials, frost and dew formation, and the observed membrane temperature convergence every night. In addition to the present

data and discussion, there is a brief description of the future work currently being done with the data and validating a temperature model.

Author

Matthew Dupuis is an engineer and researcher with Structural research Inc. (SRI) in Middleton WI. He has worked for SRI for over 10 years conducting building envelope design, forensic investigations, research projects and instruction. He holds multiple engineering degrees from the University of Wisconsin.

Introduction

During the summer of 2009, the Midwest Roofing Contractors Association (MRCA) initiated a test bed project to investigate temperature variations on low-slope roof membranes with thin-film photovoltaic (PV) panels adhered to them. The test site is located in Manhattan, Kan., at the offices of Diamond Roofing and is scheduled to last three years.

The roof was configured with seven different roof membranes from five different manufacturers. Table 1 outlines the membranes present at this site. Photos 1and 2 show a view of the roof.

Membrane Type	Color	Thickness
EPDM	White	60 mils
TPO	White	60 mils
Polymer-modified bitumen	White	140 mils
EPDM	Black	60 mils
TPO	White	60 mils
PVC	Gray	45 mils
TPO	White	60 mils

Table 1. List of membranes present and instrumented at the Manhattan, Kansas test site

Photo 1. Overhead view of the test site roof.

Each of the membranes has a thermocouple under the field membrane and under the adhered PV panel. This layout is repeated on the East and West facing slopes of the roof.

Photo 2. Roof top view of the test site roof.

Experimental

Each roof membrane type was outfitted with Type T thermocouples in the field of the membrane and thermocouples under the attached PV panels—one set on the east slope and one set on the west slope—for a total of four thermocouples per membrane. The thermocouples were placed directly under the membrane and above the top layer of insulation.

Five additional thermocouples were placed across the transition from TPO membrane to PV panel. The thermocouples were spaced apart every 2 inches. This positioned the thermocouples 4 inches under the TPO, 2 inches under the TPO, directly under the transition TPO to the PV panel, 2 inches under the PV panel and 4 inches under the PV panel.

One thermocouple was positioned under the roof deck to record the building's interior temperature.

For temperature acquisition, the National Instruments Compact RIO real-time data acquisition back plane was chosen (NI-cRIO 9073). For thermocouple readings, a pair of National Instruments 16 channel thermocouple modules were installed (NI 9213). The data acquisition system (DAQ) is connected to a desktop computer via standard TCP/IP over a 10/100 network

To drive the DAQ and record the data, software is required. Lab View 8.6.1 Full Development System was selected and installed on a desktop computer. Then, using the Lab View software a virtual instrument (VI) was programmed to acquire data from each of the 32 channels, wait for a user specified time delay before the next reading and loop again. At the end of each 24-hour period, the VI creates a data file that contains the readings. This file then can be opened and manipulated in a spreadsheet program such as Microsoft Excel.

For weather data acquisition, a commercial weather station package was selected. The Davis Instruments Vantage Pro 2 Plus weather station was used. The weather station was augmented with an aerated radiation shield for the air temperature and relative humidity sensors. The rooftop-mounted weather station receives power and transmits data via a six-conductor twisted pair hard wire back to a readout console. This console is connected to the desktop computer via USB cable, transferring the weather data to the computer. Therefore, weather data and temperature data are recorded against the system clock of the computer.

After the first year of data collection, several clear phenomena were observed in the data. The phenomenon of interest in this paper is nighttime cooling of the roof membrane. This phenomenon is related directly to the radiative exchange between the night sky, terrestrial radiation and the roof surface. This radiative exchange has been studied for building surfaces (Goodman 1938; Hoglund, Mitalas et al. 1967; Michell and Biggs 1979) and built-up roof systems (Cullen 1963), and others have looked more specifically into the nighttime cooling of intentionally ponded roof systems (Clark 1981; Yannas 2006). Another has commented on it through discussion of moisture issues related to cool roof systems (Rose 2007).

To accurately quantify and study the radiative exchange taking place between roof membranes and the environment, sensors beyond thermocouples were needed.

Sensors to measure and record the radiation exchange were installed during summer 2010.

A class 1 pyranometer and pyrgeometer from Hukseflux, the SR11 and IR02 respectively, were acquired and in July 2010 these instruments were installed on the roof at the Manhattan, Kansas site. Appropriate data acquisition modules were installed into the cRIO DAQ back plane, and the Lab View VI was modified to record the new data channels of the voltage and calculated radiation values.

Theory

Variable Definitions

q''_{net} = Net heat flux per unit area ($\frac{W}{m^2}$)

$q''_{conduction}$= Conductive heat flux per unit area ($\frac{W}{m^2}$)

$q''_{convection}$= Convective heat flux per unit area ($\frac{W}{m^2}$)

$q''_{radiation}$ = Radiative heat flux per unit area ($\frac{W}{m^2}$)

k = Thermal conductivity ($\frac{W}{m \cdot K}$)

T_I = Interior surface temperature (K)

T_S = Roof Surface Temperature (K)

L = Roof system Thickness (m)

$h_{Convection}$ = Convective heat transfer coefficient ($\frac{W}{m^2 \cdot K}$)

T_A = Ambient air temperature (K)

P = Power emitted from a radiant body ($\frac{W}{m^2}$)

σ = Stefan – Boltzmann constant 5.6704 x 10^{-8} $\frac{J}{s \cdot m^2 \cdot K^4}$

T = Temperature of radiant body (K)

ϵ = Emissivity

T_{Sky}= Apparent sky temperature (K)

E_{Solar}= Solar irradiation ($\frac{W}{m^2}$)

E_{Sky}= Sky irradiation ($\frac{W}{m^2}$)

$E_{Terrestrial}$= Terrestrial irradiation ($\frac{W}{m^2}$)

$\boldsymbol{M_{Surface}}$ = Roof surface radiant emittance

The components of heat transfer between a surface and its environment is well-documented in text books such as *Fundamentals of Heat and Mass Transfer* (Incropera, DeWitt et al. 2007). These components are conduction, convection and radiation. Each plays a part in the continuous energy exchange that occurs with the roof membrane. The most basic form of the heat transfer equation for a roof system is as follows:

$$q''_{net} = q''_{conduction} + q''_{convection} + q''_{radiation} \quad (1)$$

In this equation, q''_{net} is the net unit heat flux in watts per square meter. This is a summation of the energy arriving and leaving the roof surface. If the q''_{net} is positive, the roof system is gaining energy and temperature should rise; if the net flux is negative, the temperature should fall.

Looking specifically at the conduction term, we simply can say it is the heat energy transferred between the exterior roof surface and interior surface under the roof system. This heat energy flows through solid materials that make up the roof system and structure. This flow of heat energy is subject to thermal conductivity (k) a material property. Setting aside issues such as contact resistance and thermal bridging, we typically compute an average summation of one-dimensional, through-thickness, total conductivity for a roof system. The conduction term takes the form of:

$$q''_{Conduction} = \frac{\mathrm{k}\,(T_I - T_{S)}}{\mathrm{L}} \quad (2)$$

The convection term relates to the transfer of heat energy via the movement of fluids over the roof surface. In this specific case, we only consider air movement. The basic terms for this component involve the roof surface temperature (T_S), ambient air temperature (T_A) and a convective co-efficient ($h_{Convection}$) that accounts for factors such as the object's geometry, fluid's density, boundary layers, laminar flow, turbulent flow, etc. The general form of the convective heat flux is shown in Equation 3.

$$q''_{Convection} = h_{Convection}(T_S - T_A) \quad (3)$$

The convective co-efficient typically is determined in one of three ways: a theoretical approach, wind tunnel testing or model fitting from field data. Almost every roof system is unique in its shape, orientation, slope, edge condition, height off the ground, etc. As such, each roof system generally is unique, and a single simplified solution is not advised. Therefore, to determine the convective co-efficient, we should not use a theoretical approach because of each roof system's uniqueness and complexity. The wind tunnel method generally is impractical. Therefore, we typically will have to use a fitted model of the convective co-efficient.

Several studies have addressed the issue of modeling the convective co-efficient for a full scale roof system (Jiantao, Jing et al. 2009). These studies typically return a convective co-efficient model that varies with wind speed.

It should be noted that when the wind is not blowing the convection shifts to a passive heat transfer based on buoyancy of hot and cold air developed at the roof surface. Again, this issue is complicated by the roof orientation and design; cold air will be trapped by parapet walls and contained much like water in a glass. Therefore, a unified model for passive, buoyancy-based convection for low-slope roof systems should be approached with caution.

The radiation term has a strong influence on the heat transfer taking place during daylight hours. Incoming solar load is concentrated in the 300-2,800 nanometer range of the electromagnetic spectrum. This range is composed of ultraviolet light, visible light and short-wave infrared. It commonly is referred to as just short wave (SW). It is no coincidence the SR11 pyranometer is sensitive to this exact spectral range and therefore measures the total incoming global solar radiation.

The solar load is not the only incoming radiation the roof system receives. All matter above absolute zero emits infrared radiation. This includes oxygen, nitrogen, carbon dioxide, water vapor, dust, pollutants and other substances that make up our atmosphere. The atmosphere absorbs some of the short-wave solar load passing through it. It also absorbs the infrared energy emitted by the Earth's surface. The atmosphere then emits energy back as infrared in the 4,500 - 50,000 nanometer range; this range commonly is referred to as long-wave infrared and represents the sensitivity of the IR02 pyrgeometer, measuring incoming long-wave infrared. This incoming long-wave infrared radiation is reaching the roof surface day and night. At night, in the absence of incoming solar load, variations in the incoming long wave strongly influence how quickly a roof cools each night and how low the surface temperature drops.

Equation 4 shows the Stefan-Boltzmann law. This law relates the energy emitted by a surface in Watts per square meter to the temperature of that object in kelvin. This equation is in the form for a blackbody, and the sky typically is considered a blackbody. Using a pyrgeometer, the energy emitted from the atmosphere is converted into an effective sky temperature: T_{sky}. In the absence of a pyrgeometer to record the precise incoming long wave, several relations have been proposed; the most commonly referenced is proposed by (Berdahl and Martin 1984) and is shown for reference in Equation 5. The equation relates the sky temperature to air temperature, dew point temperature and hour after midnight. Parties interested in the derivation of variables and units for Equation 5 should review the cited work, it is shown here only as an example.

$$P = \sigma T^4 \qquad (4)$$

$$T_{Sky} = T_{Air}[0.711 + 0.0056T_{DP} + 0.000073T_{DP}^2 + 0.013\cos(15t_{midnight})]^{\frac{1}{4}} \quad (5)$$

The roof membrane is subject to equation 4, as well, and emits long-wave infrared radiation. However, it is not a blackbody. It is considered a gray body and subject to a measured emissivity (ε) value. Emissivity is a ratio of the ability of the material to emit infrared radiation compared to a perfect radiator or blackbody. Equation 4 takes the form of Equation 6 for gray bodies. This is the radiative energy emitted by the roof surface.

$$P = \epsilon\sigma T^4 \quad (6)$$

At this point, we have incoming solar short-wave irradiation, incoming long-wave sky irradiation and outgoing long-wave roof surface radiant emittance that are combined in equation 7.

A brief address should be made to the concept of terrestrial infrared radiation and its effect on a roof system. Terrestrial radiation is that which is emitted by the earth's surface, buildings, trees and other earth-based objects. This too must follow the law of all matter above absolute zero emitting infrared radiation. If we were looking at walls or steep-slope roof systems, this source of infrared irradiance should be included in our equations. However, in this case, we are looking at steep-slope roof systems that have little or no projected area exposed to terrestrial sources. Therefore, it is stricken from Equation 7 moving to Equation 8. Of additional note would be parapet walls and their effect on the terrestrial irradiance. They effectively cut off any incoming terrestrial

radiation; therefore, we would expect lower observed temperatures with parapets present.

Although the instruments and data extend 24 hours, in this study we only are concerned with nighttime effects, after the sun has set and incoming short-wave solar radiation goes to zero, as seen in Equation 8. Then, a common simplification is made (Incropera, DeWitt et al. 2007) that the roof surface is only sensitive to the spectral ranges of energies it is emitting. Therefore, we can assign the incoming long-wave sky radiation the same emissivity value as the roof, leading to Equation 9.

$$q''_{radiation} = E_{Solar} + E_{Sky} + E_{Terrestrial} - M_{Surface} \quad (7)$$

$$q''_{radiation} = E_{Sky} - M_{Surface} = \sigma {T_{Sky}}^4 + \epsilon\sigma {T_S}^4 \quad (8)$$

$$q''_{radiation} = \epsilon\sigma(T_S - T_{Sky})^4 \quad (9)$$

We then collect all the terms for equation 1 and substitute to arrive at Equation 10. This equation represents the nighttime cooling of the roof surface.

$$q''_{net} = \frac{\mathrm{k}\,(T_I - T_S)}{\mathrm{L}} + h_{Convection}(T_S - T_A) + \epsilon\sigma(T_S - T_{Sky})^4 \quad (10)$$

Results

There currently is hundreds of days' worth of data available for review. For expedience, two days randomly were selected from August 2010 for display and discussion. These days are Aug. 11, 2010, and Aug. 30, 2010. On each of these days, two charts were developed—one chart for the general array of membranes present on the roof system

and the other chart relating to the aforementioned transition array from photos 3 and 4. These charts are labeled as Chart 1 through Chart 4.

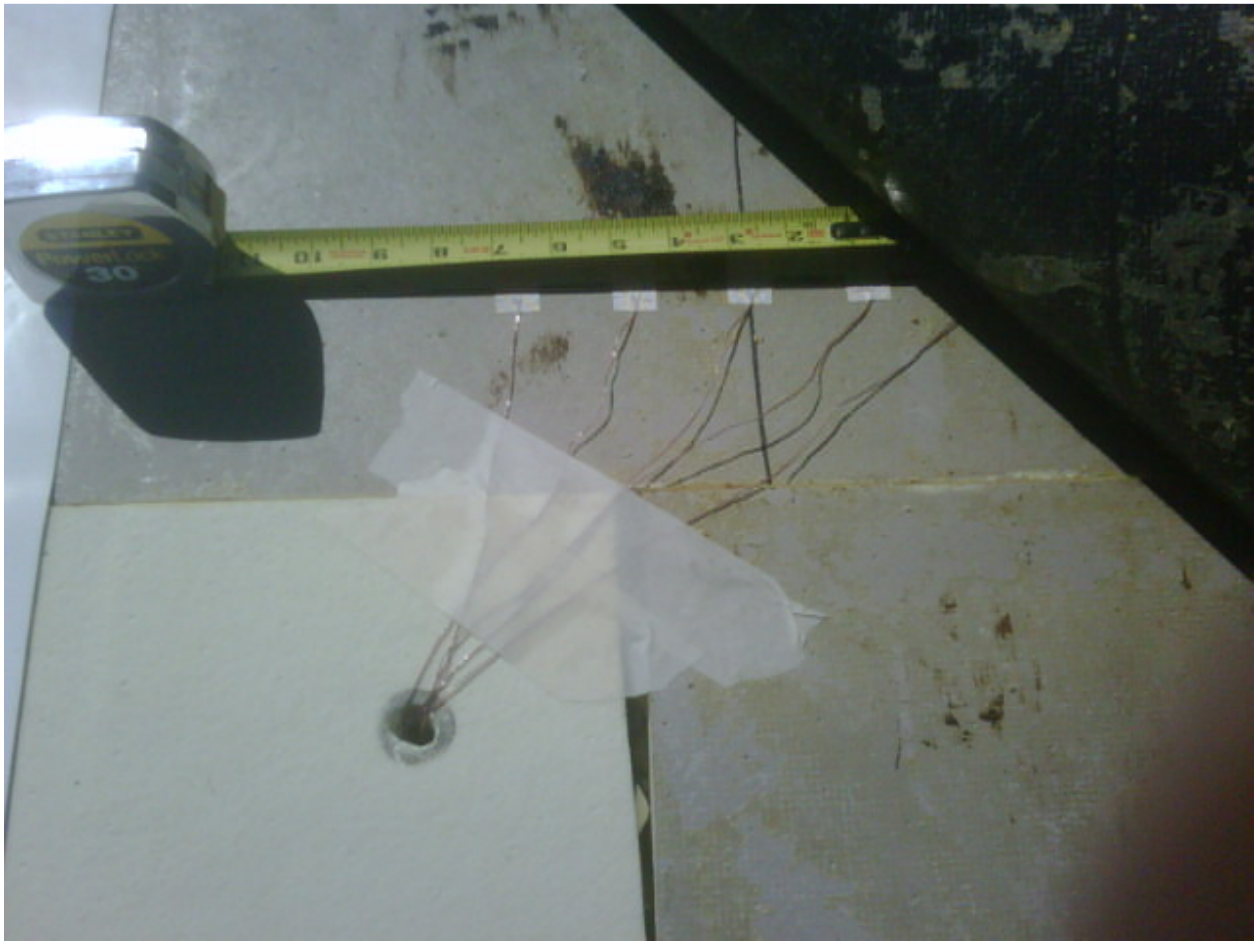

Photo 3. View of the thermocouple array, during installation, which traverses from white TPO to under the PV panel as diagramed in Photo 4.

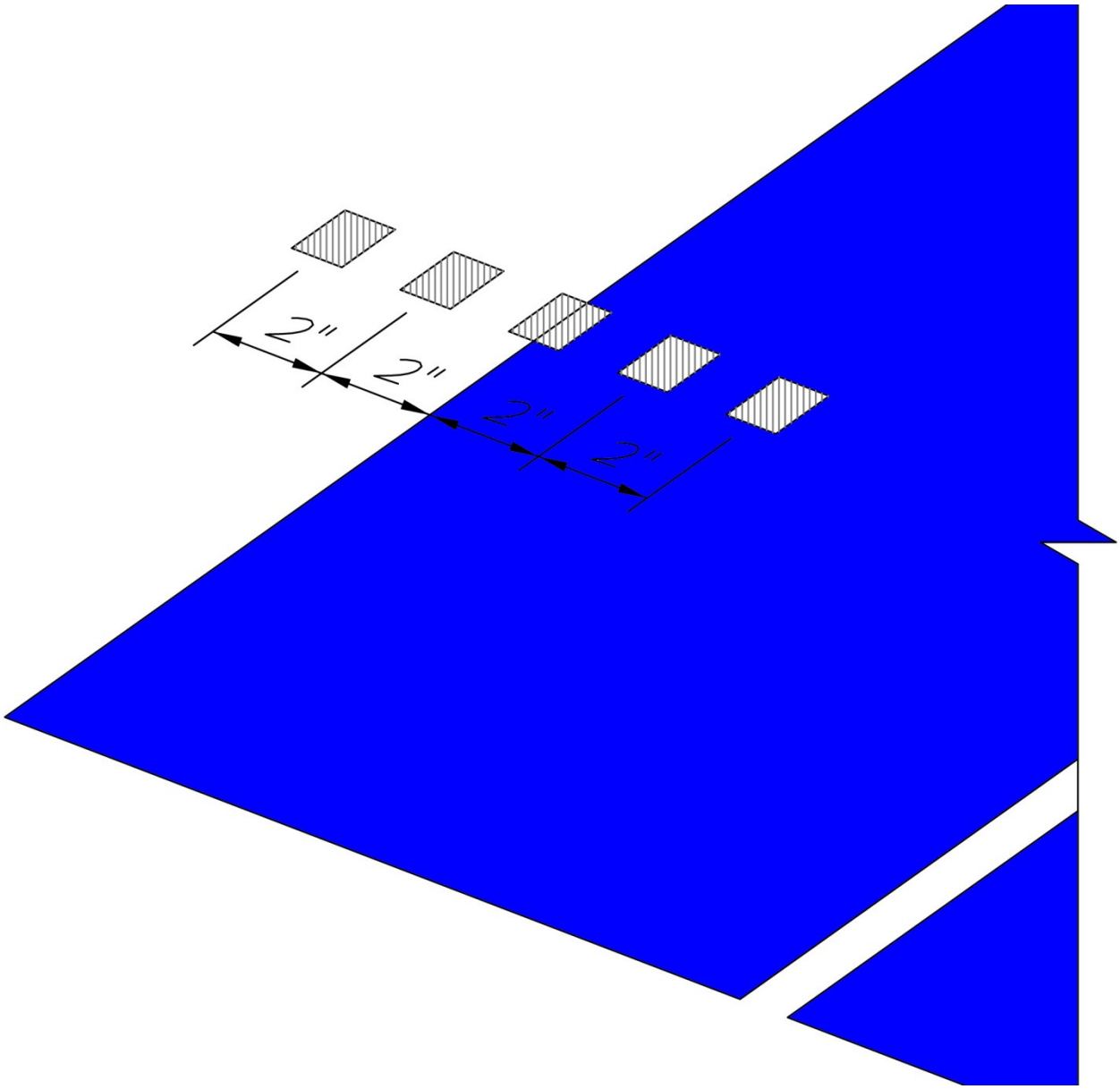

Photo 4. Diagram of the thermocouple layout that transitions from white TPO to under the PV panel.

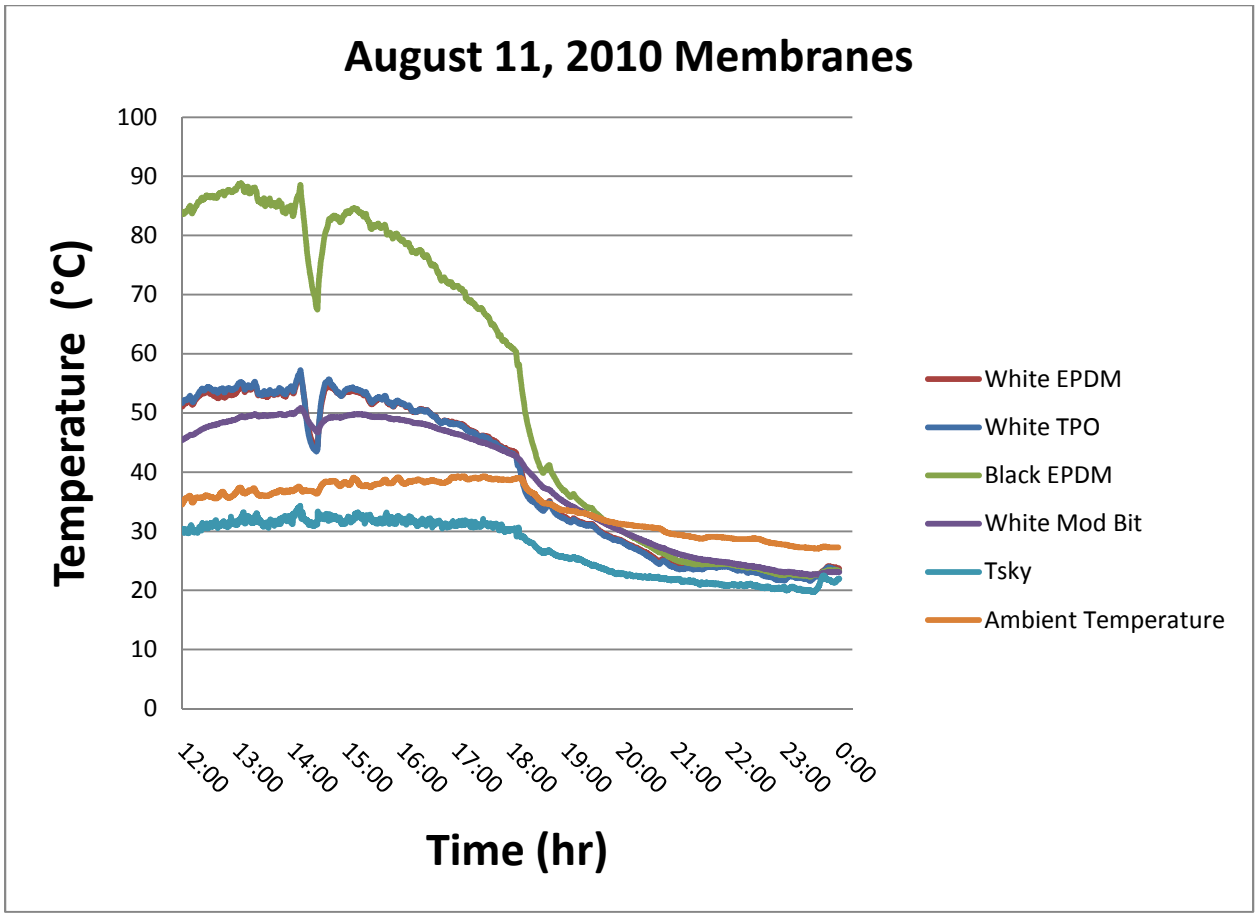

Chart 1. A 12 hour evening cycle for the roof systems. The different systems drop below the ambient air temperature at different times, but they all eventually do. The White TPO and White EPDM trace almost an identical temperature and are difficult to distinguish between the two.

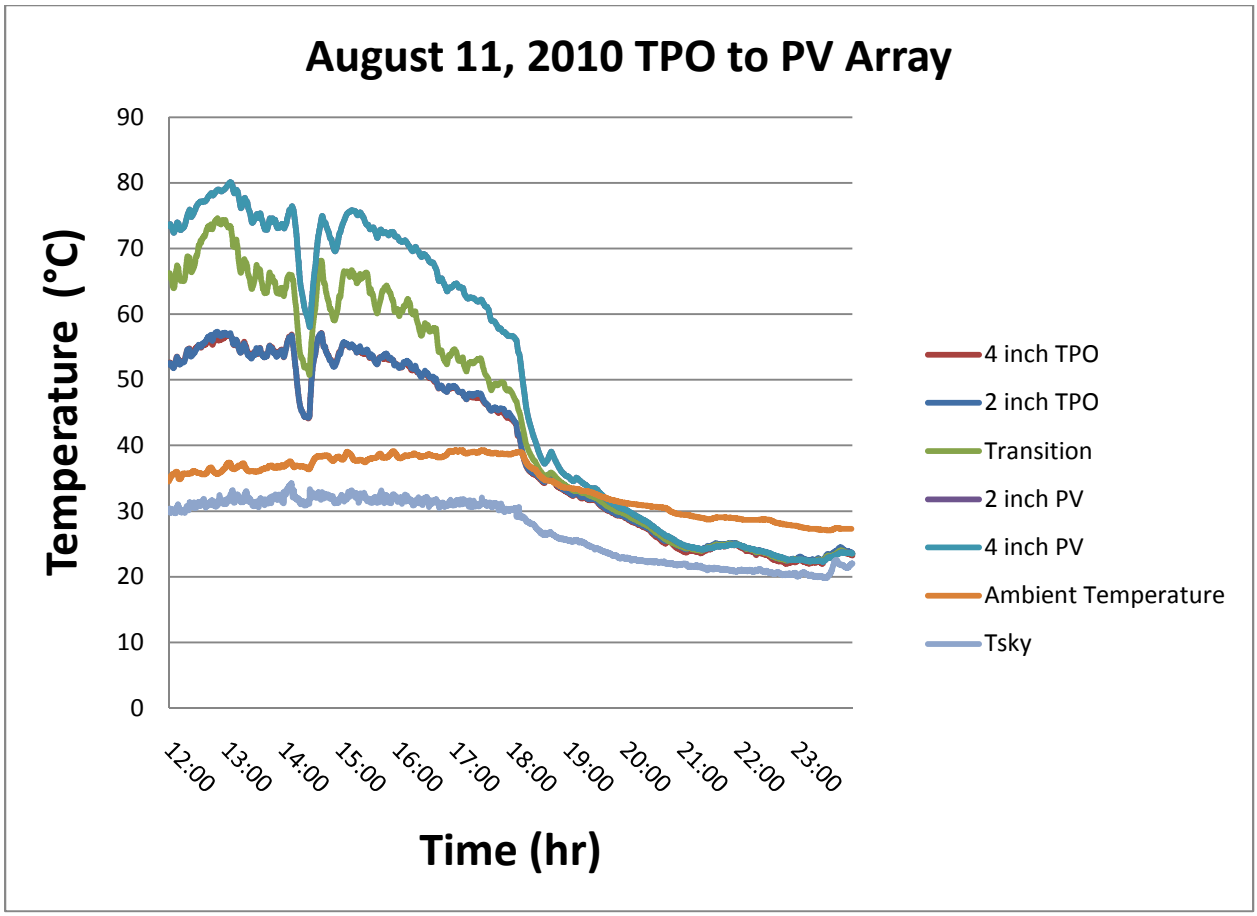

Chart 2. A 12 hour evening cycle for the TPO to PV transition array. As with the roof systems displayed in Chart 1, the TPO and PV panel drop below ambient air temperature at different points in time, but they both do. The 2 inch TPO and 4 inch TPO trace almost the exact same temperatures, as do the 2 inch PV and 4 inch PV; as such the traces are generally indistinguishable on this chart.

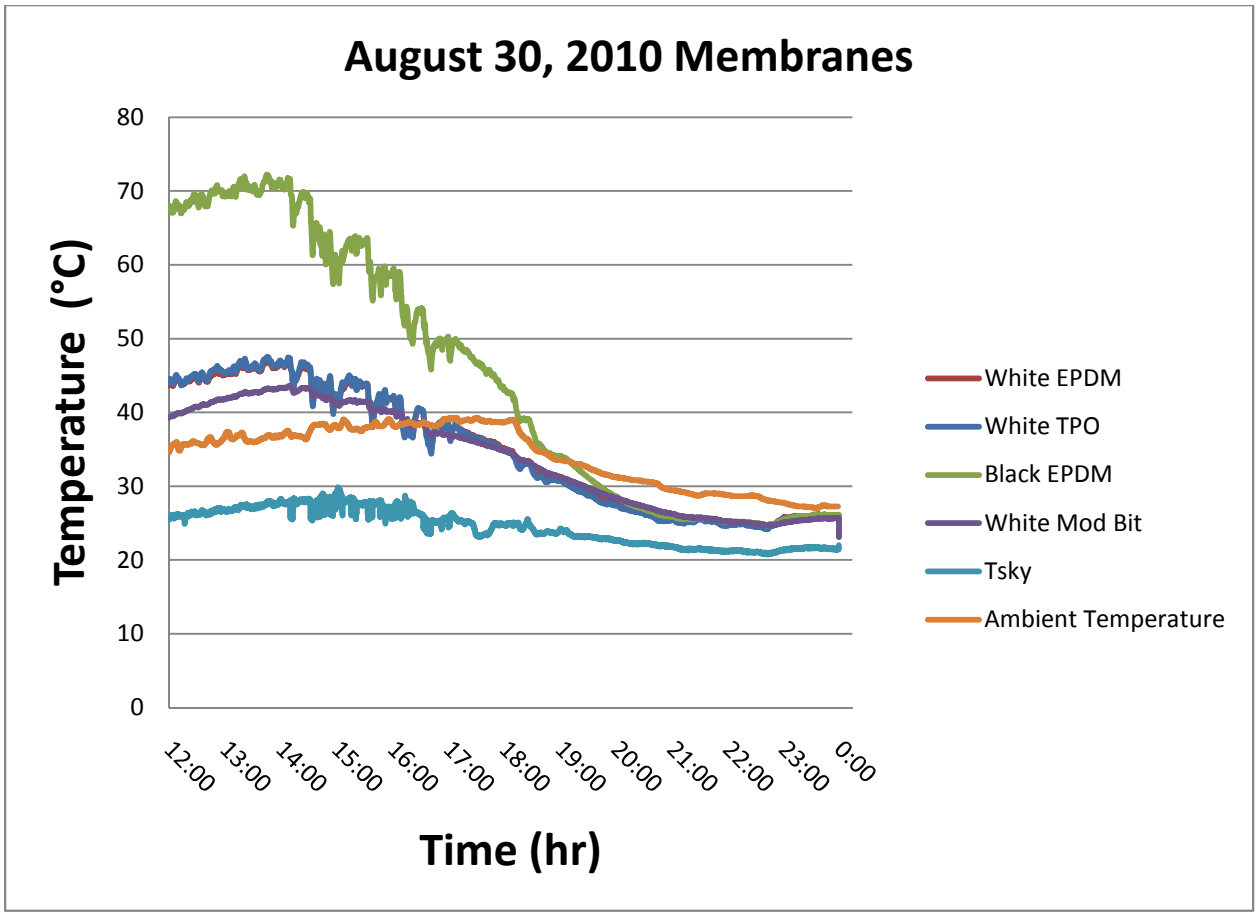

Chart 3. A 12 hour evening cycle for the roof systems. A different day with a unique data set, yet we see the same phenomena of all the roof systems dropping below the ambient air temperature. The White TPO and White EPDM trace almost an identical temperature and are difficult to distinguish between the two.

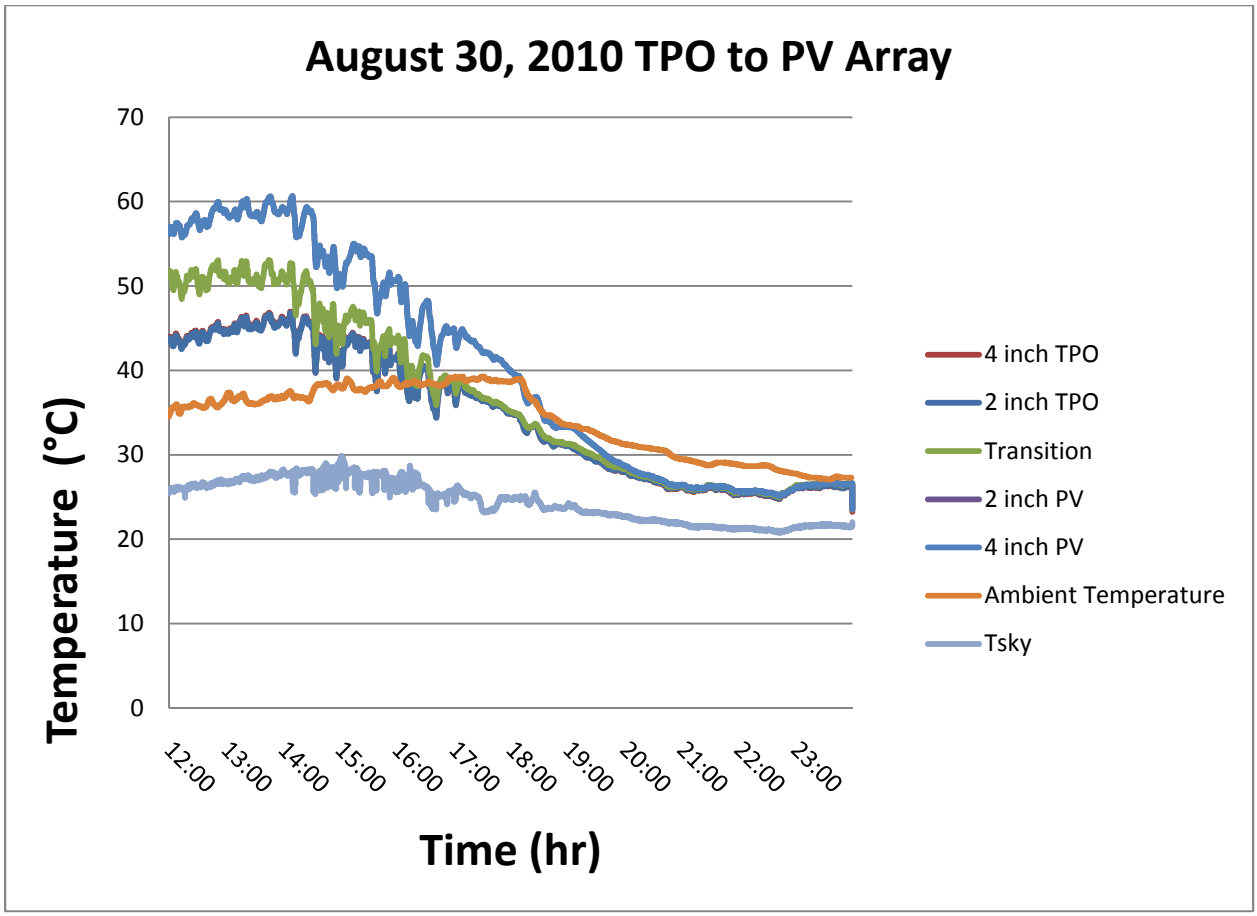

Chart 4. A 12 hour evening cycle for the TPO to PV transition array. As with the previous charts, we have a different and unique data set and the phenomena of membranes cooling below the ambient air temperature occurs. Compared to Chart 2, the inversion of ambient air to roof systems temperature occurs much earlier in the evening. The 2 inch TPO and 4 inch TPO trace almost the exact same temperatures, as do the 2 inch PV and 4 inch PV; as such the traces are generally indistinguishable on this chart.

In addition to the August data, a day from November 2010 randomly was selected from the available data sets. The same membrane types in Chart 1 and Chart 3 are displayed in Chart 5; the data in Chart 5 is presented in a different manner. The data displayed on Chart 5 starts at noon Nov. 26, 2010, and ends at noon Nov. 27, 2010. This chart effectively shows a complete nighttime cycle for the roof system.

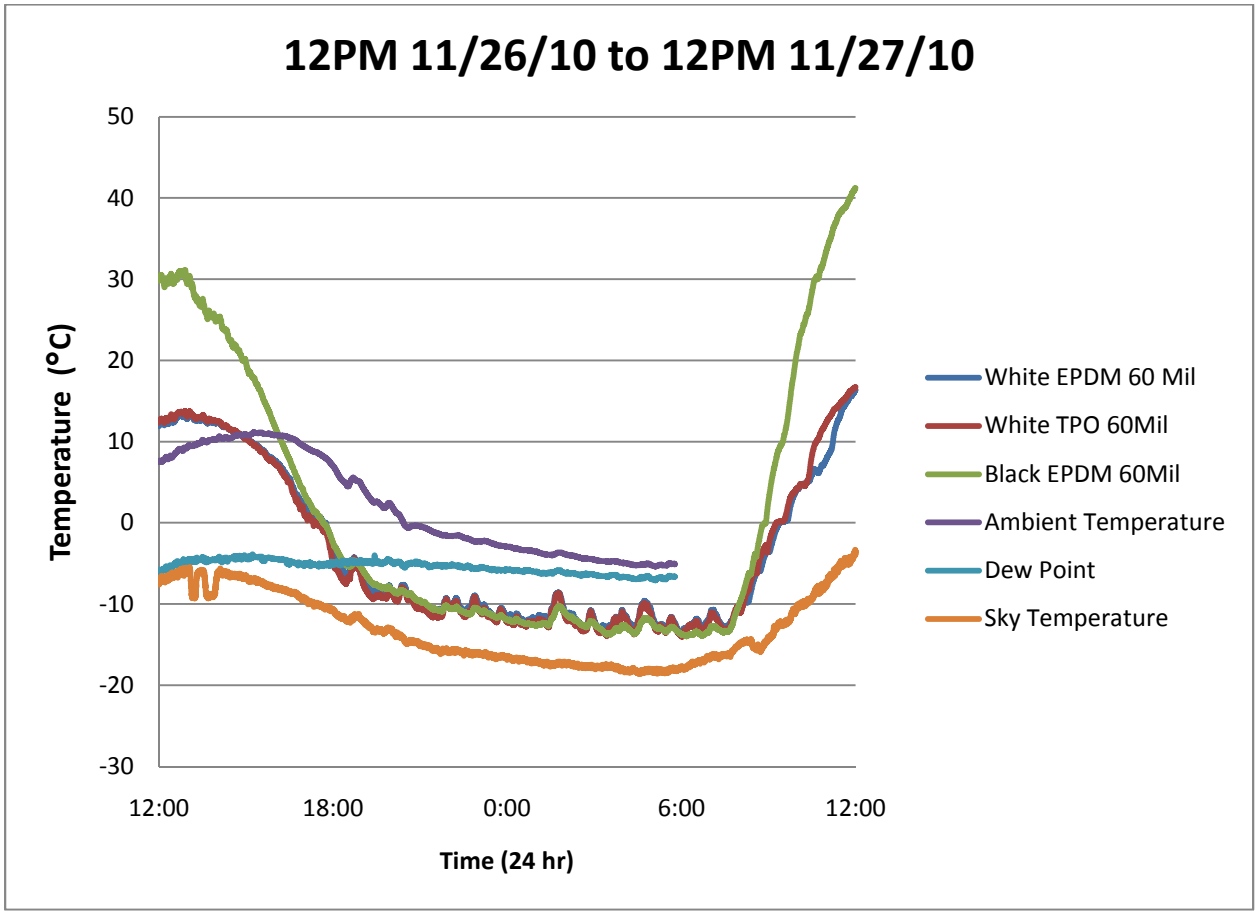

Chart 5. A full 24 hour cycle is displayed. All roof systems drop below ambient air temperature and the calculated dew point. Frost is expected to form on the roof surface.

Discussion

In Charts 1 through 5, we can see a nighttime temperature differential (ΔT) develop between the ambient air temperature and roof surface temperature, membranes or PV. In Charts 1 through 4 from August, we find a typical temperature differential of 5 C. Looking at Chart 5 from November, we find the temperature differential of slightly more than 10 C develops.

This temperature differential difference is expected. The source of the differences in nighttime cooling rates generally depends on the long-wave irradiance received from the atmosphere, related by the apparent sky temperature (Tsky). As previously discussed, sky temperature will vary with ambient air temperature and moisture present in the atmosphere (equation 5). Moisture in the air, near ground level, easily can be measured by relative humidity. However, this methodology cannot be used when cloud cover exists. The clouds will provide additional emission of infrared and reflect some terrestrial emissions back to the roof surface. This fact cannot be accounted for in approximations of the long-wave irradiance, such as equation 5. Fortunately, the pyrgeometer directly measures the total global irradiance in the long wave—it is not an approximation.

The apparent sky temperature in Chart 1 in August reaches a minimum of slightly less than 20 C while the corresponding ambient air temperature is about 27 C for a 7-degree Celsius difference. In Chart 5 in November, we find a minimum apparent sky temperature of almost -19 C and corresponding ambient air temperature of -5 C for a 14-degree Celsius difference. Why is the difference larger in November? The answer lies in the previous discussion about moisture in the air and relative humidity. The

nighttime cooling of a roof surface will be greater with dry air and a clear sky versus humid air and cloud cover. Review the results previously mentioned, temperature differential of 5 C in August and temperature differential of slightly more than 10 C in November. But it is expected that the cooling ability of humid summer air is less than that of dry, late fall air.

The data represented in Charts 1 through 5 randomly were selected from hundreds of days of data sets. Many other days' worth of data have been charted and reviewed. With the exception of when a roof system is snow-covered, the roof surface temperature has been observed to fall below ambient air temperature every night. The same statement can be made for the adhered PV panels.

The theoretical effect of the snow cover is beyond this paper's scope. However, it can be said from observation that when roof snow cover exists, the temperatures seen on any snow-covered sensor location is at or near 0 C, even though the ambient air temperature may be well above or below this temperature.

Looking at the data represented in Chart 5, we find a phenomenon of interest. The calculated dew point is shown in Chart 5. The ambient air temperature never drops below the dew point, but the membranes do, resulting from the radiative cooling. Furthermore, the dew point is below 0 C. Therefore, frost growth on roof membranes is expected.

This presents two problems for the heat transfer equation developed (equation 10). First is the fact that the frost changes the surface properties from roof membrane to ice. This will affect absorption, reflectivity and emissivity. The second problem is energy consumed in the formation of the ice crystals—enthalpy of fusion. Neither of these

situations is accounted for, and a more elaborate solution would be needed to account for this, as well as when the frost melts and/or dew evaporates, again consuming energy that would need to be taken into account.

The last point of discussion is one of observation; regardless of the membranes' color, material and solar properties, they all generally are equal during nighttime hours. The black EPDM and PV films rise to the highest temperatures during daytime hours under the sun's irradiance. However, they are able to radiate energy rapidly and thus cool rapidly because of temperature raised to the fourth power in Equation 6. Eventually the darker membranes will track together with the "cool" membranes at night.

Conclusion

The theory discussed above is not new. Many works and texts have examined it, going back to earlier parts of the 20th century. However, this work is original in that it has recorded detailed roof membrane temperatures against weather and radiometric data at the same geographic location.

Of the issues presented here, one conclusion should be clear from the charts and discussion—the service envelope for roof membranes is lower than local ambient air temperatures recorded in weather data. This work has shown roof membrane temperatures 10-degrees Celsius below ambient temperature, and this may not be the largest differential recorded in the data as the charted dates were randomly selected from the population of data sets.

Future Work

The MRCA test bed project continues to collect data 24 hours per day. Current work is under way to expand upon equation 10 and validate it against the actual temperature data recorded at the MRCA site.

However, to fully model the membranes' temperature changes, several key attributes and the test bed roof will need to be measured. Efforts currently are under way to determine the roof system's convective heat transfer co-efficient. In addition, the specific heat capacity of the membranes present at the MRCA facility will need to be determined. A differential scanning calorimeter at Madison-based University of Wisconsin's College of Engineering is being used for this purpose.

References

Berdahl, P. and M. Martin (1984). "Emissivity of Clear Skies." *Solar Energy* 5(663).

Clark, G. (1981). "Simple Estimation of Temperature and Nocturnal Heat Loss for a Radiantly Cooled Roof Mass." *Passive Cooling*: 224-244.

Cullen, W. C. (1963). Solar Heating, Radiative Cooling and Thermal Movement - Their Effects on Built-Up Roofing. U. S. D. o. C.-N. B. o. Standards. Technical Note 231.

Goodman, W. (1938). "Figuring solar heat gains of buildings." *Heating, Piping and Air Conditioning* 10(10): 657-659.

Hoglund, B. I., G. P. Mitalas, et al. (1967). "Surface temperatures and heat fluxes for flat roofs." *Building Science* 2(1): 29-36.

Incropera, DeWitt, et al. (2007). *Fundamentals of Heat and Mass Transfer*, Wiley.

Jiantao, S., L. Jing, et al. (2009). "A novel method for full-scale measurement of the external convective heat transfer coefficient for building horizontal roof." *Energy and Buildings* 41(Copyright 2009, The Institution of Engineering and Technology): 840-847.

Michell, D. and K. L. Biggs (1979). "RADIATION COOLING OF BUILDINGS AT NIGHT." *Applied energy* 5(Compendex): 263-275.

Rose, W. B. (2007). White Roofs and Moisture in the US Desert Southwest. Buildings X.

Yannas, S. (2006). *Roof Cooling Techniques a Design Handbook*, Earthscan.